MNRAS **000**, 1–8 (2016) Preprint 11 January 2017 Compiled using MNRAS LATEX style file v3.0

Suzaku spectroscopy of the neutron star transient 4U 1608–52 during its outburst decay.

M. Armas Padilla[1,2,3⋆], Y. Ueda,[3], T. Hori[3], M. Shidatsu[4] and T. Muñoz-Darias[1,2]
[1] *Instituto de Astrofísica de Canarias (IAC), Vía Láctea s/n, La Laguna 38205, S/C de Tenerife, Spain*
[2] *Departamento de Astrofísica, Universidad de La Laguna, La Laguna, E-38205, S/C de Tenerife, Spain*
[3] *Department of Astronomy, Kyoto University, Kitashirakawa-Oiwake-cho, Sakyo-ku, Kyoto 606-8502, Japan*
[4] *MAXI Team RIKEN, 2-1 Hirosawa, Wako, Saitama 351-0198, Japan*

arXiv:1701.02728v1 [astro-ph.HE] 10 Jan 2017

Accepted XXX. Received YYY; in original form ZZZ

ABSTRACT

We test the proposed 3-component spectral model for neutron star low mass X-ray binaries using broad-band X-ray data. We have analysed 4 X-ray spectra (0.8–30 keV) obtained with *Suzaku* during the 2010 outburst of 4U 1608–52, which have allowed us to perform a comprehensive spectral study covering all the classical spectral states. We use a thermally Comptonized continuum component to account for the hard emission, as well as two thermal components to constrain the accretion disc and neutron star surface contributions. We find that the proposed combination of multicolor disc, single-temperature black body and Comptonization components successfully reproduces the data from soft to hard states. In the soft state, our study supports the neutron star surface (or boundary layer) as the dominant source for the Comptonization seed photons yielding the observed weak hard emission, while in the hard state both solutions, either the disc or the neutron star surface, are equally favoured. The obtained spectral parameters as well as the spectral/timing correlations are comparable to those observed in accreting black holes, which support the idea that black hole and neutron star low mass X-ray binaries undergo a similar state evolution during their accretion episodes.

Key words: accretion, accretion discs – stars: individuals (4U 1608–52) – stars: neutron star – X-rays: binaries

1 INTRODUCTION

Stellar-mass black holes (BHs) and numerous neutron stars (NSs) are revealed when they form part of low mass X-ray binaries (LMXBs), where they are accreting material from a low mass ($< M_\odot$) companion star. Accretion takes place via an accretion disc (Shakura & Sunyaev 1973), whose inner regions are viscously heated up to $\sim 10^{6-7}$ K, making these sources the brightest in the night X-ray sky. Depending on the accretion rate, LMXBs can be found in two flavours, transient and persistent sources. The former spend most part of their lives in a faint, quiescent state at X-ray luminosities $L_X \sim 10^{30-32}$ erg s^{-1}, but show occasional outburst – that can last several months – when brightness increases over a million fold. Persistent systems are always active (i.e. in outburst), with $L_X > 10^{36}$ erg s^{-1} (but see Armas Padilla et al. 2013).

Given the rather comparable binary system parameters and gravitational wells, it is not always straightforward to distinguish between NS and BH accretors in LMXBs. A definitive proof for a BH is obtained when the compact object mass exceeds $3M_\odot$ (e.g. Casares & Jonker 2014), the maximum stable mass of a NS in general relativity (Rhoades & Ruffini 1974; Kalogera & Baym 1996). In absence of dynamical measurements, NSs are confirmed by events associated with the presence of a solid surface and magnetic field (absent in BHs), such as thermonuclear X-ray burst and coherent pulsations, respectively. From the X-ray point of view, BH-LMXBs are simpler objects with two main spectral components: (i) a hard component believed to arise from inverse-Compton processes in an optically thin inner flow (corona) and typically modelled with a power-law, and (ii) a soft, thermal accretion disc component. The evolving balance between them lead to the presence of the so-called *hard* and *soft* accretion states, which alternate following well-defined hysteresis patterns (e.g. Miyamoto et al. 1992, 1995) in the spectral and variability domains (Homan et al. 2001; Done et al. 2007; Muñoz-Darias et al. 2011; Belloni et al. 2011, for a review).

In NS-LMXBs, the X-ray emission from the solid surface

⋆ e-mail: m.armaspadilla@iac.es

© 2016 The Authors

and/or boundary layer (hereafter, we will refer this as NS surface for simplicity) is expected to contribute to the X-ray spectrum, in addition to the aforementioned hard (comptonizing corona) and soft (accretion disc) spectral components. This lead to a more complex spectral evolution and state phenomenology (Hasinger & van der Klis 1989; van der Klis 2006). Nevertheless, BH and NS-LMXBs are known to have very similar timing properties (e.g. Wijnands & Van Der Klis 1999). Recently, BH-like hysteresis paths (Muñoz-Darias et al. 2014) have been found to be a common feature also in NS systems accreting at sub-Eddintong rates (a.k.a. atoll sources).

Since the dawn of X-ray astronomy many efforts have been made to model the NS-LMXBs spectra. In the 80s, two models using differing approaches were proposed, and dubbed *Eastern* (Mitsuda et al. 1984, 1989) and *Western* (White et al. 1988) models. Both include two components, but they differ on their physical origin. On one hand, the *Eastern* model attributes the soft emission to the accretion disc and the hard component to Comptonization of seed photons emitted on the NS surface. In the *Western* model, on the other hand, the NS surface and the Comptonized disc are the sources of the soft and hard components, respectively (see Barret 2001 for a review). Along the years, both approaches have been successfully applied. As an example, Done et al. (2002), fitted the same Cyg X-2 data with both methods, obtaining statistically indistinguishable results. Besides model degeneracy, it is not either clear whether any the above methods can be consistently (i.e. keeping the same physical meaning for every component) describe the spectral evolution through the different stages (states) of an outburst. Moreover, given the overall similarity between LMXBs with NS and BH accretors, the large database now available for both groups, and the spectral simplicity expected for the latter, a BH oriented approach could potentially lead to more general conclusions.

Lin et al. (2007, hereafter LRH07) tested the two above scenarios and end up proposing a *hybrid*, 3-component model. These are, (i) a constrained broken power-law (CBPL), (ii) a multi-color disc model(MCD) and (iii) a single-temperature blackbody (BB), which account for the Comptonization, the accretion disc and NS surface emissions, respectively. This solution is able to model the spectra of two transient NS-LMXBs (see also Lin et al. 2009 for an extension) at different states and luminosities, fulfilling physical and phenomenological constraints typically observed in BH systems (see Section 3.2). Likewise, by combining this modelling with the evolution of the fast temporal variability, a consistent BH-NS accretion state picture is found even for the brightest NS-LMXBs (a.k.a. Z sources). This includes similar accretion-outflow coupling properties for both families (Muñoz-Darias et al. 2014; Fender & Muñoz-Darias 2015, for a review).

One of the limitations of the LRH07 study is the lack of coverage at energies $\lesssim 3$ keV (they used *RXTE* data), which hampered a detailed modelling of the thermal components (disc and NS surface). This is particularly troublesome in the hard state, when these are weaker. As a matter of fact, LRH07 found that the accretion disc component was not required to fit the hard state observations, a limitation commonly suffered in BH systems when using the same instrumentation (e.g., Muñoz-Darias et al. 2013). However, hard state discs are detected in the same BHs when observing with instruments providing lower energy coverage (e.g. Plant et al. 2015; De Marco et al. 2015).

In this paper we take the LRH07 approach as the starting point to analyse 4 broad-band (0.8–30 keV) *Suzaku* observations covering the 2010 outburst decay of 4U 1608–52 from soft to hard states. This source, one of the two used to test the aforementioned spectral model, is a well-known transient NS-LMXB (Grindlay & Gursky 1976; Tananbaum et al. 1976), which recurrently undergoes into outburst (e.g. Negoro et al. 2014). From radius-expansion type I X-ray burst the distance is estimated to be in the range 3.2–4.1 kpc (Nakamura et al. 1989; Galloway et al. 2008), and the detection of rapid oscillation in some of these events indicates that the NS spins at 620 Hz (Muno et al. 2001). 4U 1608–52 has been extensively studied, with works published on its X-ray variability properties (e.g. Yoshida et al. 1993; Altamirano et al. 2008; Barret 2013), burst episodes (e.g. Galloway et al. 2008; Poutanen et al. 2014), disc reflection features (e.g. Degenaar et al. 2015) and spectral properties (e.g. Gierlinski & Done 2002; Asai et al. 2012, LRH07). The latest group, however, was mostly carried out with data from instruments with a coverage-lack at low energies, which results in strong limitations when modelling the soft components; a caveat that can be accounted for by using *Suzaku* data.

2 OBSERVATIONS AND DATA REDUCTION

4U 1608–52 was observed with the spacial facility *Suzaku* (Mitsuda et al. 2007) during its 2010 outbourst. Four observations were performed throughout the outburst decay, on 2010 March 11, 15, 18 and 22, for a total observing time of ∼114 ksec (see Figure 1). We used the HEASOFT v.6.18 software and *Suzaku* Calibration Database (CALDB) released on 2015 March 12 for the reduction and analysis of our data. After reprocessing the data with the *Suzaku* `FTOOL` `aepipeline` and removing burst events present in observations 404044020 and 404044030, we followed the *Suzaku* ABC guide[1] to obtain the final data products.

The X-ray Imaging Spectrometer (XIS; Koyama et al. 2007) was operated in the 1/4 window mode and using the burst option to avoid pile-up effects (see Table1 for the observation log). We used a circular region with a radius of 110″centred on the system position to extract the source events, and a circular region of the same size placed in a source-free part of the CCDs to extract the background. The XIS response matrix and ancillary response files were created using `xisrmfgen` and `xisarfgen` tasks. We made use of the `aepileupcheckup.py` script developed by Yamada et al. (2012) to evaluate the pile-up fraction in our observations. It returned an estimation of less than 2% at the core of the PSFs. Nevertheless, to ensure that our spectral results are not affected by pile-up, we extracted the source spectra using several annular regions excluding photons coming from the most central region. The spectra are consistent with each other confirming that the pile-up effect is negligible. We

[1] `http://heasarc.gsfc.nasa.gov/docs/suzaku/analysis/abc/`

Table 1. *Suzaku* observations log.

Observations		Date		XIS		HXD-PIN
(Obs)	ID	MJD	yyyy-mm-dd	Burst option	Net exposure[a]	Net exposure[a]
1	404044010	55266.07	2010-03-11	0.13 sec	2.2 ksec	28 ksec
2	404044020	55270.69	2010-03-15	0.13 sec	2.3 ksec	25.1 ksec
3	404044030	55273.99	2010-03-18	0.5 sec	7.8 ksec	14.1 ksec
4	404044040	55277.98	2010-03-22	1.0 sec	15.9 ksec	14.5 ksec

[a] Exposure time per sensor after dead-time and burst events substration.

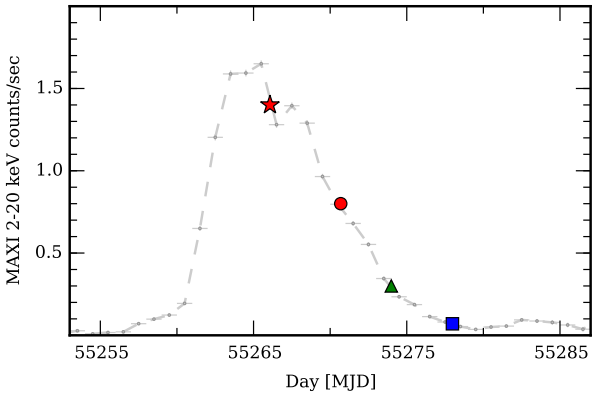

Figure 1. The 2010 outburst light curve (2-20 keV) of 4U 1608–52 obtained by *MAXI*. The times of the 4 *Suzaku* observations are indicated by the coloured symbols. Observation 1, 2, 3, and 4 are indicated by a red star, a red circle and a blue square, respectively. Same symbol/colour code is used for all the figures.

combined spectra and response files of the two frontside-illuminated cameras (FI-XISs; XIS-0 and XIS-3) with the `addascaspec` task to maximize the signal-to-noise ratio. The spectra from the backside-illuminated camera XIS-1 was excluded from our study due to discrepancies (probably by inaccurate cross calibration) with the FI-XISs, which are more sensitive at high energies.

We extracted the spectra from PIN silicon diodes of the Hard X-ray Detector (HXD; Takahashi et al. 2007) using the `FTOOL hxdpinxbpi` provided by the *Suzaku* team. This script produces the background spectrum extracting the non-X-ray background (NXB) from the tunned background modeled by the HXD team, and adding the contribution of the cosmic X-ray background (CXB) following the Boldt (1987) recipe. Due to the Galactic coordinates of the source (l=330.92°, b=-0.85°), we also account for contamination caused by Galactic ridge X-ray emission following Revnivtsev et al. (2003, 2006). In our analysis we used the appropiate response file provided on the *Suzaku* CALDB. The source was not significantly detected with the Gadolinium Silicate (GSO) scintillator.

2.1 Rossi X-ray Timing Explorer

The four *Suzaku* observations were (at least) partially covered by simultaneous *Rossi X-ray Timing Explorer* (RXTE) data. In Fig. 2 we present both the hardness-intensity and rms-intensity diagrams (HID and RID, respectively) from Muñoz-Darias et al. (2014). These include every (980) RXTE pointing of 4U 1608–52 during its $\sim$15 years of operations. Every RXTE observation is represented by a grey dot. Observations simultaneous with the *Suzaku* data are highlighted using the same colour code as in Fig. 1. The RID was performed following Muñoz-Darias et al. (2011) by computing fractional root-mean-square (rms) in the 0.1–64 Hz frequency band. In the HID, *Hardness* was defined as the ratio of counts between the 10–16 keV and 6–10 keV bands, respectively. RXTE net count-rate (Y axis in Fig. 2) is computed in the band 2–15 keV. Hard states are found at rms $\gtrsim$ 15 % and hardness $\gtrsim$ 0.6, whilst soft states are characterized by rms $\lesssim$ 5 % and hardness $\lesssim$ 0.4 (see Muñoz-Darias et al. 2014, for further details).

3 ANALYSIS AND RESULTS

We used XSPEC (v.12.9, Arnaud 1996) to analyse our spectra. We added a 1 per cent systematic error to every spectrum to account for calibration uncertainties (Makishima et al. 2008), and excluded both the 1.7-1.9 keV and 2.2-2.4 keV energy ranges to avoid the silicon K-edge and gold M-edge calibration uncertainties, respectively. In order to deal with cross-calibration issues we added a constant factor (CONSTANT) to the spectral models with a value fixed to 1 for XIS spectra and 1.16 for HXD spectra [2]. We included the photoelectric absorption component (PHABS) to account for the interstellar absorption assuming the cross-sections of Balucinska-Church & McCammon (1992) and the abundances of Anders & Grevesse (1989). Finally, the 1-10 keV FI-XISs and 15-30 keV HXD/PIN spectra were simultaneously fitted by using tied spectral parameters. We note that HXD/PIN data above 30 keV were excluded since they do not exceed the background level (at 3σ).[3]

In this paper we aim at modelling 4 *Suzaku* spectra using the LRH07 3-component model. The broader energy range (particularly in the soft band) of our data allow us to give an step forward with respect to previous works. On one hand, and differently from LRH07 who used a (constrained) broken power-law to model the hard component, we utilize a more physically meaningful thermally Comptonized continuum component (NTHCOMP in XSPEC; Zdziarski et al. 1996; Zycki et al. 1999). On the other hand, we apply the very same 3-component model also to the hard state spectrum (obs. 4), contrastingly to the simpler 2-component approach proposed in the hybrid model. Thus, we use the model DISKBB+BBODYRAD+NTHCOMP in XSPEC to fit

[2] Suzaku Memo 2008-06 at `http://www.astro.isas.jaxa.jp/suzaku/doc/suzakumemo`

[3] The 40-70 keV NXB have a 3σ systematic error of 8.4-5.4% for an exposure of 10-20 ksec, respectively (Fukazawa et al. 2009)

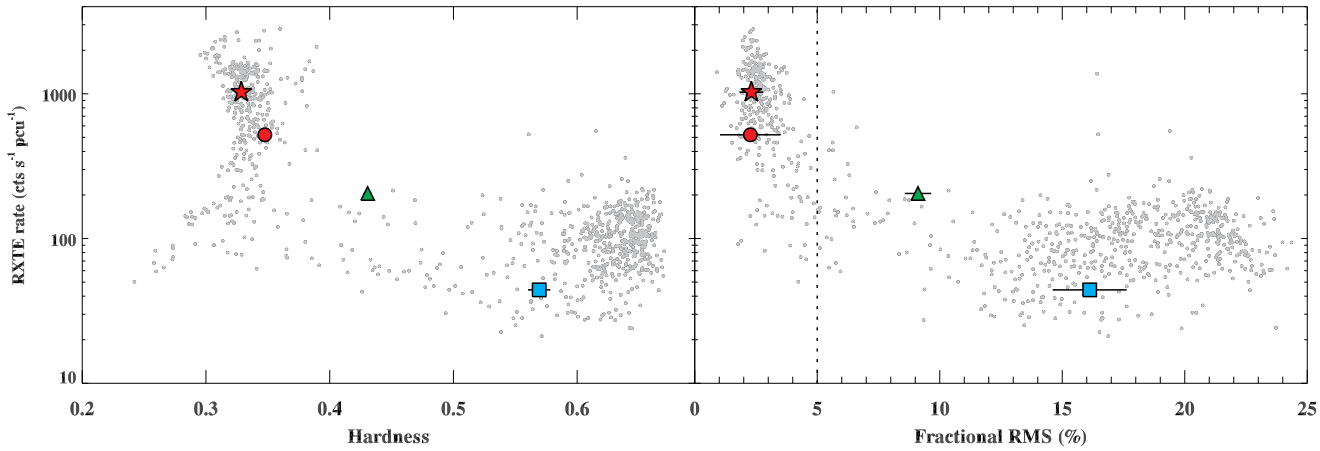

Figure 2. Hardness intensity diagram (left panel) and rms intensity diagram (right panel) of 4U 1608–52 using RXTE observations (see text). Data simultaneous to our *Suzaku* campaign are highlighted using the same colour scheme as in Fig. 1. The Dashed line represents the 5 % variability level, which roughly define the soft states in BH and NS LMXBs. Adapted from Muñoz-Darias et al. (2014).

soft (obs. 1 and 2), intermediate (obs. 3) and hard (obs. 4) state data of the same source taken during the same outburst. Results are reported in Table 2 and Fig. 3 with uncertainties given at 90 per cent confidence level.

We have two possible seed-photon solutions for the Comptonized emission. One assumes that the up-scattered photons arise from the disc and the second associates them with the NS surface. Thus, we coupled $KT_{\rm seed}$ to either $KT_{\rm disk}$ or $KT_{\rm bb}$, respectively, and changed the seed photons shape parameter accordingly (*im_type* in NTHCOMP; see Table 2). Both approaches yield statistically indistinguishable results (χ^2_ν<1.05). In Table 2, we report only the case in which the seed photons arise from the NS surface (see Section 4 for discussion). On the other hand, given the complexity of the modelling, uncertainties have been calculated in two steps, that is, freezing the thermal components when calculating the error associated with the hard tail (NTHCOMP) and vice versa.

We note that, in contrast to previous studies of the low state spectra where a reflection component was required (e.g, Yoshida et al. 1993 using *Ginga* data; Degenaar et al. 2015 using *NuSTAR*), our modelling do not require reflection related features. As a test, we added to our models a Gaussian component in order to search for the presence of a Fe-K line with central energy of 6.4 keV and a width of 0.1 keV, consistently with previous works (e.g. LRH07). We always found upper limits as stringent as Fe-K equivalent width < 14eV. Therefore, the reflection features from a cold outer disk are either absent or buried by the continuum.

3.1 Spectral parameters

Spectral fits yield a hydrogen column density ($N_{\rm H}$) of $\sim 1\times10^{22}$cm^{-2}, which agrees with values previously reported (Penninx et al. 1989; Güver et al. 2010). The inferred 0.8–30 keV unabsorbed flux goes from 13.8×10^{-9}erg cm^{-2} s^{-1} in the soft state, to 0.6 $\times10^{-9}$erg cm^{-2} s^{-1} in the hard state. Assuming a distance of 3.6 kpc, they translate into a luminosity drop from 21.5 to 0.9 $\times10^{36}$erg s^{-1} (0.1 to 0.004 $L_{\rm Edd}$ assuming an Eddington luminosity of $L_{\rm Edd}$=2×10^{38}erg s^{-1}). The soft-to-hard transition occurs at $\sim$ 0.02 $L_{\rm Edd}$, which agrees with the 0.01-0.04 $L_{\rm Edd}$ range proposed by Maccarone (2003) for this transition in BH and NS LMXBs.

The disc and NS temperatures behave as expected for the corresponding accretion rates, since they drop from 1 to 0.2 keV and from 1.6 to 0.4 keV, respectively. From the black body normalization we infer an emission radius ($R_{\rm bb}$) in the range of $\sim$1–6 km, which is consistent with previous works (e.g., Sakurai et al. 2014). These small $R_{\rm bb}$ values can be interpreted as resulting from emission from a boundary layer taking the shape of an equatorial belt (LRH07 and references therein; see also Matsuoka & Asai 2013). We note, however, that it is not straightforward to obtain physically meaningful $R_{\rm bb}$ values from this kind of modelling. Also, we did not apply any correction for the photons scattered by the Corona which might increase the obtained values by a factor <2 (see Kubota et al. 2004).

Finally, the (Comptonization) asymptotic power-law photon index (Γ) slightly decreases as the flux goes down, from $\sim$2.3 to 2, whereas the electron corona temperature ($KT_{\rm e}$) increases from 3.3 to 18 keV. These values correspond to a decrease on the electron scattering optical depth (τ) from $\sim$ 8 to $\sim$3 [4]. The thermal components contribute by $\sim$ 77 per cent to the total luminosity in the soft state ($\sim$ 54 per cent from the disc and 23 per cent from the NS surface). On the contrary, the thermal contribution is only $\sim$15 per cent in the hard state .

3.2 Some initial sanity tests

LRH07 approached model degeneracy by setting a number of physical evaluation criteria. These are:
1. The inner disc radii have values comparable/higher than the size of the NS.

[4] Photon index is related to kT_e and optical depth (τ) through the relation $\Gamma = \alpha + 1 = \left[\frac{9}{4} + \frac{1}{(kT_e/m_ec^2)\tau(1+\tau/3)}\right]^{1/2} - \frac{1}{2}$ (Sunyaev & Titarchuk 1980; Lightman & Zdziarski 1987)

2. The thermal components (MCD and BB) roughly evolve as $L_X \propto T^4$.
3. The disc temperature is lower than the NS surface temperature ($KT_{diskbb} < KT_{bb}$; Mitsuda et al. 1989; Popham et al. 2001); and therefore the seed photons temperature should not exceed the NS surface temperature ($KT_{seed} \leqslant KT_{bb}$).
4. The Comptonization fraction is consistent with the power density spectrum, assuming that in NS-LMXBs the X-ray variability changes as a function of spectral hardness similarly to the BHs systems.

In order to test the first condition we converted the normalization of the disc component (N_{diskbb}) into inner disk radius (R_{in}) following the relation:

$$R_{in} = \xi\,\kappa^2 \left(\frac{N_{disk}}{cos\ i}\right)^{0.5} \frac{D}{10\ \mathrm{kpc}}\ [\mathrm{km}] \quad (1)$$

(Kubota et al. 1998; Gierlinski & Done 2002). D is the source distance, i is the disc inclination angle, κ is the ratio of color temperature to effective temperature (Shimura & Takahara 1995), and ξ is the correction factor for the inner torque-free boundary condition (Kubota et al. 1998), although we note that the torque-free boundary condition is most likely not fulfilled in NS-LMXBs. Here we adopt κ=1.7 , ξ=0.4 and $i = 70°$. The obtained inner disc radii are in the range R_{in} ∼15–45 km. These values become slightly smaller (R_{in} ∼11–30 km) if $i = 40°$(Degenaar et al. 2015), but are in any case larger than the expected NS radius (e.g. Lattimer & Prakash 2000; Zdunik & Haensel 2012). These values are consistent with those obtained by Degenaar et al. (2015), which use a reflection model to fit a 4U 1608–52 *NuSTAR* observation at ∼0.02 L_{Edd} (i.e. similar to those consider here).

Condition 3 is also fulfilled (see Table 2), while Condition 4 is discussed in Section 4 since it has important implications on the nature of the Comptonized emission. Finally, Condition 2 only makes sense if the inner disc radius is constant with time. We observe than both the black-body and the disc components roughly evolved as $L_X \propto T^4$ (not showed), which is consistent with the rather small variation measured in the inner radius. Nevertheless, the reader should bear in mind that our disc radius measurements are derived from a Newtonian model (DISKBB) and should be taken with caution when used for more complex calculations.

3.3 Hard state observation

We have successfully fitted the hard state observation (Obs. 4) with the 3-component model. We tried also the simpler 2-component approach, which includes the Comptonization component and only one of the thermal emissions (either MCD or BB). We find that the DISK+NTHCOMP model fits adequately the data with χ^2= 1487 and 1403 dof . The corresponding spectral parameters are shown in the last column of Table 2 and the fit itself (red dashed line) in the last panel of Fig. 3. On the other hand, the BB+NTHCOMP model results in $\chi^2$of 1507 and soft residuals are observed. Statistically speaking, the former approach is consistent with the null hypothesis at 5 per cent significance level (p=0.057), while it is rejected by the latter one. Therefore, we find that both the 3-component model and a simplified version of it (DISK+NTHCOMP) are able to reproduce the data. Even if degeneracy is obviously an issue, we note that an F-test indicates that the 3-component model ($\chi^2$of 1445 with 1400 dof.) is significantly better. In addition, the obtained spectral parameters follow the same trend than for the previous 3 observations, suggesting that this modelling provides a realistic description of the spectral evolution of the system.

4 DISCUSSION

Model degeneration is a fundamental problem when studying the spectral evolution on NS-LMXBs. Here, we take advantage of the broad-spectral coverage and good spectral resolution of *Suzaku* to test the 3-component model proposed by LRH07 as part of the *hybrid model*. To this end, we have used 4 observations of the NS-LMXB 4U 1608–52 taken during its 2010 outburst decay, covering the soft-to-hard transition (two in the soft state [SS], one in the intermediate state [IS] and one in the hard state [HS]).

Our 3-component model combines MCD, BB and NTHCOMP, which account for the emission from the accretion disc and NS surface, and the Comptonization contribution, respectively. Using this model we have successfully fit all four observations, obtaining spectral parameters which are within typical ranges from previous studies on 4U 1608–52 (e.g. Gierlinski & Done 2002; Lin et al. 2007; Degenaar et al. 2015) and other NS LMXBs (e.g. Done et al. 2002; Lin et al. 2009; Takahashi et al. 2011; Sakurai et al. 2012).

The evolution of each component through the different accretion states could be interpreted according to the following picture: In the soft state, most of the emission is produced by the the NS surface and the accretion disc (which probably extends close to the NS surface) and only a little amount of radiation (∼ 20%) is produced by Comptonization of seed photons emitted by these components. As accretion drops, the disc temperature and its associated luminosity decrease, which might be a consequence of disc truncation. Following this drop in accretion rate, there is a subsequent decrease on the NS surface temperature and luminosity. Thus, the Comptonization emission starts to be dominant, and eventually becomes the main source of emission in the hard state. This simplistic picture is similar to what is seeing in BH-LMXBs, with the difference that for NS systems an additional soft component is required to account for the NS surface. The presence of this extra thermal radiation should have an important role in producing the Comptonized emission.

4.1 The nature of the Comptonized emission

So far we have discussed results obtained by assuming that the main source of seed photons for the Comptonization process is the NS surface (or boundary layer; i.e. we coupled KT_{seed} with KT_{bb}). However, good fits are also obtained when assuming that the disc is the main source of seed photons (fifth column in Table 2). Indeed, the obtained temperatures and photon indices are in the range expected for NS-LMXBs. Fig. 4 shows the evolution of the fractional rms as function of the thermal luminosity fraction for both possible seed photon solutions. When comparing the two approaches, the first striking thing is that the thermal fraction drops to ∼40 per

Table 2. Fitting results for the DISKBB+BBODYRAD+NTHCOMP model for the 4 observations assuming that seed-photons arise from the NS surface ($KT_{\rm seed}$ tied to $KT_{\rm bb}$). The fifth column shows the results for obs.4 with the same model but assuming that seed-photons arise from the disc ($KT_{\rm seed}$ tied to $KT_{\rm in}$). Last column shows the results for obs. 4 using the simpler DISKBB+NTHCOMP model ($KT_{\rm seed}$ tied to $KT_{\rm in}$). Both spectra and models are shown in Fig. 3. Uncertainties are expressed at 90 per cent confidence level.

Component	Obs1 (SS)	Obs2 (SS)	Obs3 (IS)	Obs4 (HS)	Obs4 (HS) alternative models	
					seed photons (DISKBB)	(DISKBB+NTHCOMP)
$N_{\rm H}$ ($\times10^{22}$cm^{-2})	1.07±0.01	1.05±0.01	1.01±0.02	0.99±0.15	1.1±0.1	1 (fix)
$KT_{\rm in}$ (keV)	1.00±0.006	0.92±0.006	0.621±0.004	0.23 ±0.02	0.15±0.01	0.40±0.02
$N_{\rm diskbb}$	448±10	386±10	623±17	4160^{+2046}_{-1346}	53694^{+70658}_{-25350}	140^{+27}_{-13}
$KT_{\rm bb}$ (keV)	1.63±0.004	1.70±0.006	1.25±0.005	0.395±0.001	0.42±0.01	–
$N_{\rm bb}$	40±1.2	21.2±0.7	14.7±0.6	277± 27	143±22	–
Γ/τ [a]	2.26±0.06/7.69	2.18±0.1/7.8	2.14±0.03/3.53	1.98±0.01/3.23	1.98±0.01/3.15	2.03±0.02
$KT_{\rm e}$ (keV)	3.31±0.09	3.2 ±0.1	$14.5^{+6.5}_{-2.9}$	18^{+14}_{-4}	19^{+14}_{-5}	999^{+29}_{-5}
imp_type	0	0	0	0	1	1
$N_{\rm nthcomp}$ ($\times10^{-2}$)	3.16±0.06	1.44 ±0.04	1.71±0.02	5.11 ±0.04	12.3±0.1	9.8±0.7
$F_{\rm X}$[b] (erg cm^{-2} s^{-1})	14.20±0.06	8.33±0.05	3.09±0.03	0.76±0.02	0.83±0.04	0.76±0.02
$L_{\rm X}$[c] (erg s^{-1})	2.20±0.01	1.29 ±0.01	0.479±0.005	0.118±0.003	0.128±0.006	0.118±0.003
MCD fraction	54	57	41	7	3	7
BB fraction	23	23	12	8	5	–
NTHCOMP fraction	23	20	47	85	92	93
χ^2_ν /dof	0.96/1859	1.02/1324	1.03/1370	1.03/1400	1.03/1400	1.06/1403

[a] The electron scattering optical depth (τ) is obtained following the relation $\Gamma = \left[\frac{9}{4} + \frac{1}{(kT_e/m_ec^2)\tau(1+\tau/3)}\right]^{1/2} - \frac{1}{2}$

[b] Unabsorbed 0.8-30 keV flux in units of 10^{-9}erg cm^{-2} s^{-1}.

[c] 0.8-30 keV luminosity in units of 10^{37}erg s^{-1} assuming a distance of D=3.6 kpc.

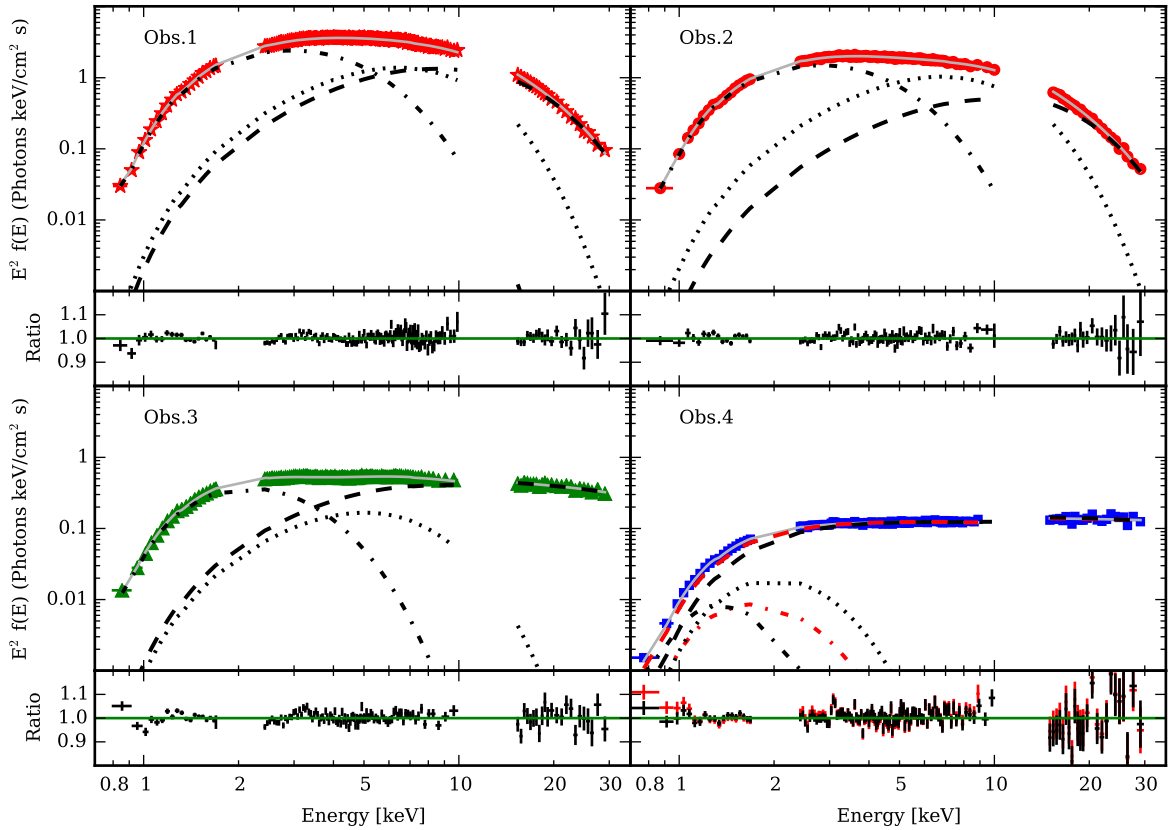

Figure 3. Unfolded spectra and data-to-model ratio using the DISKBB+BBODYRAD+NTHCOMP model. **The full fit** is shown as a solid grey line, the disc component as a dot-dashed line, the blackbody component as a dotted line and the Comptonized component as a dashed line. In the last panel the obs. 4 results obtained by using the simpler DISKBB+NTHCOMP model are overplotted in red. XIS data are re-binned in XSPEC for clarity.

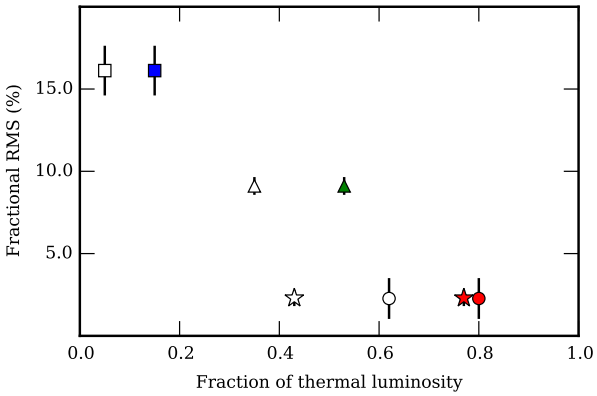

Figure 4. RMS fraction versus fraction of thermal luminosity (DISKBB+BB). Filled and empty symbols correspond to 3-component model solutions assuming that the seed photons for the Comptonized emission arise from the NS surface and the accretion disc, respectively.

cent in obs. 1, versus ∼80 per cent if the NS surface solution is adopted. The former value is much lower than that observed in BHs at the same variability levels (note that variability is generally observed to trace the Comptonization fraction; e.g. Remillard & Mcclintock 2006). Moreover, the values obtained for the soft states observations (obs. 1 and 2) differ significantly from each other when the disc approach is used. This is at odds with the similar hardness and rms values measured, both quantities being model independent and typically used to track the evolution of the accretion flow (Fig. 2). Nevertheless, we note that, as usual, the complexity of the nature exceeds any spectral fitting and probably both NS surface and disc photons are Comptonized. Thus, it is important to bear in mind that our model is only able to favour one components as the dominant source of seed photons. On the other hand, from Fig. 4 we cannot rule out the disc as the main source of seed photons for obs. 3 and 4. Indeed, our spectral modelling with 2-components strongly suggest that, if anything, the disc component might provide the most relevant thermal contribution in the hard state.

4.2 Black holes comparative

One of the main advantages of the 3-component model is the straightforward comparison that it provides with BH-LMXBs, which show only one thermal component (i.e. the disc). Our soft state and intermediate temperatures are consistent with values typically observed in BH systems (e.g., Muñoz-Darias et al. 2013) in agreement with findings by LRH07. However, the big advantage of our *Suzaku*-based study is the ability to study the thermal components in the hard state, when these are much weaker. Plant et al. (2015) modelled hard state observations of GX 339-4, a BH transient that is seen at an intermediate orbital inclination, as it is probably the case of 4U 1608–52. They find $KT_{\rm diskbb}$ in the range 0.15–0.28 in remarkable agreement with our work ($KT_{\rm diskbb} = 0.23 \pm 0.02$). In the same way, and using *Suzaku* observations, Shidatsu et al. (2014) find a similar range of disc temperatures in the hard state of H1743–322.

Finally, we note that we do not see a strong evolution in our photon indices, which decrease from 2.3 to 2. While the former value is consistent with BH soft states ($\Gamma \sim 2$–3), values $\Gamma \lesssim 2$ are more typical for the hard state. We note, however, that our hard state observation is one of the softest of 4U 1608–52 in this state, as significantly larger rms and hardness values have been observed (see Fig. 2).

5 CONCLUSIONS

We have performed a detailed study of the spectral evolution of the neutron star X-ray transient 4U 1608–52 during the decay of its 2010 outburst. Our 0.8–30 keV *Suzaku* observations covered soft, intermediate and hard states epochs. We find that the 3-component model provides an excellent description of the outburst evolution. The inferred spectral parameters evolve in agreement with expectations, fulfilling several physical criteria, and reporting values consistent with those seen in other NS sources and in BH transients, whose spectral evolution is thought to be less complex. In the hard state, where the thermal emission is weaker and less energetic, the 3-component model is statistically preferred over simpler solutions. Likewise, we find that the disc component, typically observed in BHs when low energy coverage is available, is in any case required. Future works including more observations (e.g. at different stages of the hard state) and a variety of sources should be able to further extend this study. To this end, we note that high-quality coverage at low energies is a desired feature, especially at low fluxes.

ACKNOWLEDGEMENTS

MAP was funded by the International Research Fellowship program of the Japan Society for the Promotion of Science (PE15024). MAP and TMD acknowledge the hospitality of the Kyoto University, where part of this work was carried out. MAP acknowledge the hospitality on her visit to RIKEN, and thanks the valuable discussion with K. Makishima, T. Mihara and the other members of the MAXI team. MAP's research is funded under the Juan de la Cierva Fellowship Programme of the Ministry of Science and Innovation (MINECO) of Spain. MAP and TMD acknowledge support by the Spanish MINECO grant AYA2013-42627. MS acknowledges support by the Special Postdoctoral Researchers Program at RIKEN. This research has made use of data obtained from the Suzaku satellite, a collaborative mission between the space agencies of Japan (JAXA) and the USA (NASA).

REFERENCES

Altamirano D., van der Klis M., Méndez M., Jonker P. G., Klein-Wolt M., Lewin W. H. G., 2008, ApJ, 685, 436
Anders E., Grevesse N., 1989, Geochimica et Cosmochimica Acta, 53, 197
Armas Padilla M., Degenaar N., Wijnands R., 2013, MNRAS, 434, 1586
Arnaud K., 1996, in Jacoby G., Barnes J., eds, Astronomical Society of the Pacific Conference Series Vol. 101, Astronomical Data Analysis Software and Systems V. p. 17

Asai K., et al., 2012, PASJ, 64, 128
Balucinska-Church M., McCammon D., 1992, ApJ, 400, 699
Barret D., 2001, Adv. Sp. Res., 28, 307
Barret D., 2013, ApJ, 770, 9
Belloni T. M., Motta S. E., Muñoz-Darias T., 2011, Bulletin of the Astronmical Society of India, 39, 409
Boldt E., 1987, Observational Cosmology, 124, 611
Casares J., Jonker P. G., 2014, Space Sci. Rev., 183, 223
De Marco B., Ponti G., Muñoz-Darias T., Nandra K., 2015, MNRAS, 454, 2360
Degenaar N., Miller J. M., Chakrabarty D., Harrison F. A., Kara E., Fabian A. C., 2015, MNRAS Lett, 451, L85
Done C., Zycki P. T., Smith D. A., 2002, MNRAS, 331, 453
Done C., Gierlinski M., Kubota A., 2007, The Astronomy and Astrophysics Review, 15, 1
Fender R., Muñoz-Darias T., 2015, Lect. Notes Phys., 905, 65
Fukazawa Y., et al., 2009, PASJ, 61, S17
Galloway D. K., Muno M. P., Hartman J. M., Psaltis D., Chakrabarty D., 2008, ApJS, 179, 360
Gierlinski M., Done C., 2002, MNRAS, 337, 1373
Grindlay J., Gursky H., 1976, ApJ, 209, L61
Güver T., Özel F., Cabrera-Lavers A., Wroblewski P., 2010, ApJ, 712, 964
Hasinger G., van der Klis M., 1989, A&A, 225, 79
Homan J., Wijnands R., van der Klis M., Belloni T., van Paradijs J., Klein-Wolt M., Fender R., Méndez M., 2001, ApJS, 132, 377
Kalogera V., Baym G., 1996, ApJ, 470, L61
Koyama K., et al., 2007, PASJ, 59, S23
Kubota A., Tanaka Y., Makishima K., Ueda Y., Dotani T., Inoue H., Yamaoka K., 1998, PASJ, 50, 667
Kubota A., et al., 2004, ApJ, 601, 428
Lattimer J. M., Prakash M., 2000, ApJ, 550, 426
Lightman A. P., Zdziarski A. A., 1987, ApJ, 319, 643
Lin D., Remillard R. A., Homan J., 2007, ApJ, 667, 1073
Lin D., Remillard R. A., Homan J., 2009, ApJ, 696, 1257
Maccarone T. J., 2003, A&A, 409, 697
Makishima K., et al., 2008, PASJ, 60, 585
Matsuoka M., Asai K., 2013, PASJ, 65, 26
Mitsuda K., et al., 1984, PASJ, 36, 741
Mitsuda K., Inoue H., Nakamura N., Tanaka Y., 1989, PASJ, 41, 97
Mitsuda K., et al., 2007, PASJ, 59, S1
Miyamoto S., Kitamoto S., Iga S., Negoro H., Terada K., 1992, ApJ, 391, L21
Miyamoto S., Kitamoto S., Hayashida K., Egoshi W., 1995, ApJ, 442, L13
Muno M. P., Chakrabarty D., Galloway D. K., Savov P., 2001, ApJ, 553, L157
Muñoz-Darias T., Motta S., Belloni T. M., 2011, MNRAS, 410, 679
Muñoz-Darias T., Coriat M., Plant D. S., Ponti G., Fender R. P., Dunn R. J. H., 2013, MNRAS, 432, 1330
Muñoz-Darias T., Fender R. P., Motta S. E., Belloni T. M., 2014, MNRAS, 443, 3270
Nakamura N., Dotani T., Inoue H., Mitsuda K., Tanaka Y., Matsuoka M., 1989, PASJ, 41, 617
Negoro H., et al., 2014, Astron. Telegram
Penninx W., Damen E., van Paradijs J., Tan J., Lewin W. H. G., 1989, A&A, 208, 146
Plant D. S., Fender R. P., Ponti G., Muñoz-Darias T., Coriat M., 2015, A&A, 573, A120
Popham R., et al., 2001, ApJ, 547, 355
Poutanen J., Nattila J., Kajava J. J. E., Latvala O.-M., Galloway D. K., Kuulkers E., Suleimanov V. F., 2014, MNRAS, 442, 3777
Remillard R. A., Mcclintock J. E., 2006, ARA&A, 44, 49
Revnivtsev M., Gilfanov M., Sunyaev R., Jahoda K., Markwardt C., 2003, A&A, 411, 329
Revnivtsev M., Sazonov S., Gilfanov M., Churazov E., Sunyaev R., 2006, A&A, 452, 169
Rhoades C., Ruffini R., 1974, Phys. Rev. Lett., 32, 324
Sakurai S., Yamada S., Torii S., Noda H., Nakazawa K., Makishima K., Takahashi H., 2012, PASJ, 64, 72
Sakurai S., et al., 2014, PASJ, 66, 10
Shakura N. I., Sunyaev R. A., 1973, A&A, 24, 337
Shidatsu M., et al., 2014, ApJ, 789, 100
Shimura T., Takahara F., 1995, ApJ, 445, 780
Sunyaev R. A., Titarchuk L. G., 1980, A&A, 86, 121
Takahashi T., et al., 2007, PASJ, 59, S35
Takahashi H., Sakurai S., Makishima K., 2011, ApJ, 738
Tananbaum H., Chaisson L. J., Forman W., Jones C., Matilsky T. A., 1976, ApJ, 209, L125
White N. E., Stella L., Parmar A. N., 1988, ApJ, 324, 363
Wijnands R., Van Der Klis M., 1999, Astron. Astrophys, 345, 35
Yamada S., et al., 2012, PASJ, 64, 53
Yoshida K., Mitsuda K., Ebisawa K., Ueda Y., Fujimoto R., Yaqoob T., Done C., 1993, PASJ, 45, 605
Zdunik J. L., Haensel P., 2012, A&A, 551
Zdziarski A., Johnson W., Magdziarz P., 1996, MNRAS, 283, 193
Zycki P. T., Done C., Smith D. A., 1999, MNRAS, 309, 561
van der Klis M., 2006, In: Compact stellar X-ray sources. Edited by Walter Lewin & Michiel van der Klis. Cambridge Astrophysics Series

This paper has been typeset from a TEX/LATEX file prepared by the author.